

Test of CP Symmetry in Hyperon to Neutron Decays

M. Ablikim¹, M. N. Achasov^{13,b}, P. Adlarson⁷⁵, X. C. Ai⁸¹, R. Aliberti³⁶, A. Amoroso^{74A,74C}, M. R. An⁴⁰, Q. An^{71,58}, Y. Bai⁵⁷, O. Bakina³⁷, I. Balossino^{30A}, Y. Ban^{47,g}, V. Batozskaya^{1,45}, K. Begzsuren³³, N. Berger³⁶, M. Berlowski⁴⁵, M. Bertani^{29A}, D. Bettoni^{30A}, F. Bianchi^{74A,74C}, E. Bianco^{74A,74C}, J. Bloms⁶⁸, A. Bortone^{74A,74C}, I. Boyko³⁷, R. A. Briere⁵, A. Brueggemann⁶⁸, H. Cai⁷⁶, X. Cai^{1,58}, A. Calcaterra^{29A}, G. F. Cao^{1,63}, N. Cao^{1,63}, S. A. Cetin^{62A}, J. F. Chang^{1,58}, T. T. Chang⁷⁷, W. L. Chang^{1,63}, G. R. Che⁴⁴, G. Chelkov^{37,a}, C. Chen⁴⁴, Chao Chen⁵⁵, G. Chen¹, H. S. Chen^{1,63}, M. L. Chen^{1,58,63}, S. J. Chen⁴³, S. M. Chen⁶¹, T. Chen^{1,63}, X. R. Chen^{32,63}, X. T. Chen^{1,63}, Y. B. Chen^{1,58}, Y. Q. Chen³⁵, Z. J. Chen^{26,h}, W. S. Cheng^{74C}, S. K. Choi^{10A}, X. Chu⁴⁴, G. Cibinetto^{30A}, S. C. Coen⁴, F. Cossio^{74C}, J. J. Cui⁵⁰, H. L. Dai^{1,58}, J. P. Dai⁷⁹, A. Dbeysi¹⁹, R. E. de Boer⁴, D. Dedovich³⁷, Z. Y. Deng¹, A. Denig³⁶, I. Denysenko³⁷, M. Destefanis^{74A,74C}, F. De Mori^{74A,74C}, B. Ding^{66,1}, X. X. Ding^{47,g}, Y. Ding⁴¹, Y. Ding³⁵, J. Dong^{1,58}, L. Y. Dong^{1,63}, M. Y. Dong^{1,58,63}, X. Dong⁷⁶, S. X. Du⁸¹, Z. H. Duan⁴³, P. Egorov^{37,a}, Y. L. Fan⁷⁶, J. Fang^{1,58}, S. S. Fang^{1,63}, W. X. Fang¹, Y. Fang¹, R. Farinelli^{30A}, L. Fava^{74B,74C}, F. Feldbauer⁴, G. Felici^{29A}, C. Q. Feng^{71,58}, J. H. Feng⁵⁹, K. Fischer⁶⁹, M. Fritsch⁴, C. Fritsch⁶⁸, C. D. Fu¹, J. L. Fu⁶³, Y. W. Fu¹, H. Gao⁶³, Y. N. Gao^{47,g}, Yang Gao^{71,58}, S. Garbolino^{74C}, I. Garzia^{30A,30B}, P. T. Ge⁷⁶, Z. W. Ge⁴³, C. Geng⁵⁹, E. M. Gersabeck⁶⁷, A. Gilman⁶⁹, K. Goetzen¹⁴, L. Gong⁴¹, W. X. Gong^{1,58}, W. Gradl³⁶, S. Gramigna^{30A,30B}, M. Greco^{74A,74C}, M. H. Gu^{1,58}, Y. T. Gu¹⁶, C. Y. Guan^{1,63}, Z. L. Guan²³, A. Q. Guo^{32,63}, L. B. Guo⁴², M. J. Guo⁵⁰, R. P. Guo⁴⁹, Y. P. Guo^{12,f}, A. Guskov^{37,a}, T. T. Han⁵⁰, W. Y. Han⁴⁰, X. Q. Hao²⁰, F. A. Harris⁶⁵, K. K. He⁵⁵, K. L. He^{1,63}, F. H. H. Heinsius⁴, C. H. Heinz³⁶, Y. K. Heng^{1,58,63}, C. Herold⁶⁰, T. Holtmann⁴, P. C. Hong^{12,f}, G. Y. Hou^{1,63}, X. T. Hou^{1,63}, Y. R. Hou⁶³, Z. L. Hou¹, H. M. Hu^{1,63}, J. F. Hu^{56,i}, T. Hu^{1,58,63}, Y. Hu¹, G. S. Huang^{71,58}, K. X. Huang⁵⁹, L. Q. Huang^{32,63}, X. T. Huang⁵⁰, Y. P. Huang¹, T. Hussain⁷³, N. Hüsken^{28,36}, W. Imoehl²⁸, M. Irshad^{71,58}, J. Jackson²⁸, S. Jaeger⁴, S. Janchiv³³, J. H. Jeong^{10A}, Q. Ji¹, Q. P. Ji²⁰, X. B. Ji^{1,63}, X. L. Ji^{1,58}, Y. Y. Ji⁵⁰, X. Q. Jia⁵⁰, Z. K. Jia^{71,58}, P. C. Jiang^{47,g}, S. S. Jiang⁴⁰, T. J. Jiang¹⁷, X. S. Jiang^{1,58,63}, Y. Jiang⁶³, J. B. Jiao⁵⁰, Z. Jiao²⁴, S. Jin⁴³, Y. Jin⁶⁶, M. Q. Jing^{1,63}, T. Johansson⁷⁵, X. K.¹, S. Kabana³⁴, N. Kalantar-Nayestanaki⁶⁴, X. L. Kang⁹, X. S. Kang⁴¹, R. Kappert⁶⁴, M. Kavatsyuk⁶⁴, B. C. Ke⁸¹, A. Khoukaz⁶⁸, R. Kiuchi¹, R. Kliemt¹⁴, O. B. Kolcu^{62A}, B. Kopf⁴, M. K. Kuessner⁴, A. Kupsc^{45,75}, W. Kühn³⁸, J. J. Lane⁶⁷, P. Larin¹⁹, A. Lavanina²⁷, L. Lavezzi^{74A,74C}, T. T. Lei^{71,k}, Z. H. Lei^{71,58}, H. Leithoff³⁶, M. Lellmann³⁶, T. Lenz³⁶, C. Li⁴⁸, C. Li⁴⁴, C. H. Li⁴⁰, Cheng Li^{71,58}, D. M. Li⁸¹, F. Li^{1,58}, G. Li¹, H. Li^{71,58}, H. B. Li^{1,63}, H. J. Li²⁰, H. N. Li^{56,i}, Hui Li⁴⁴, J. R. Li⁶¹, J. S. Li⁵⁹, J. W. Li⁵⁰, K. L. Li²⁰, Ke Li¹, L. J. Li^{1,63}, L. K. Li¹, Lei Li³, M. H. Li⁴⁴, P. R. Li^{39,j,k}, Q. X. Li⁵⁰, S. X. Li¹², T. Li⁵⁰, W. D. Li^{1,63}, W. G. Li¹, X. H. Li^{71,58}, X. L. Li⁵⁰, Xiaoyu Li^{1,63}, Y. G. Li^{47,g}, Z. J. Li⁵⁹, Z. X. Li¹⁶, C. Liang⁴³, H. Liang^{1,63}, H. Liang^{71,58}, H. Liang³⁵, Y. F. Liang⁵⁴, Y. T. Liang^{32,63}, G. R. Liao¹⁵, L. Z. Liao⁵⁰, J. Libby²⁷, A. Limphirat⁶⁰, D. X. Lin^{32,63}, T. Lin¹, B. J. Liu¹, B. X. Liu⁷⁶, C. Liu³⁵, C. X. Liu¹, F. H. Liu⁵³, Fang Liu¹, Feng Liu⁶, G. M. Liu^{56,i}, H. Liu^{39,j,k}, H. B. Liu¹⁶, H. M. Liu^{1,63}, Huanhuan Liu¹, Huihui Liu²², J. B. Liu^{71,58}, J. L. Liu⁷², J. Y. Liu^{1,63}, K. Liu¹, K. Y. Liu⁴¹, Ke Liu²³, L. Liu^{71,58}, L. C. Liu⁴⁴, Lu Liu⁴⁴, M. H. Liu^{12,f}, P. L. Liu¹, Q. Liu⁶³, S. B. Liu^{71,58}, T. Liu^{12,f}, W. K. Liu⁴⁴, W. M. Liu^{71,58}, X. Liu^{39,j,k}, Y. Liu^{39,j,k}, Y. Liu⁸¹, Y. B. Liu⁴⁴, Z. A. Liu^{1,58,63}, Z. Q. Liu⁵⁰, X. C. Lou^{1,58,63}, F. X. Lu⁵⁹, H. J. Lu²⁴, J. G. Lu^{1,58}, X. L. Lu¹, Y. Lu⁷, Y. P. Lu^{1,58}, Z. H. Lu^{1,63}, C. L. Luo⁴², M. X. Luo⁸⁰, T. Luo^{12,f}, X. L. Luo^{1,58}, X. R. Lyu⁶³, Y. F. Lyu⁴⁴, F. C. Ma⁴¹, H. L. Ma¹, J. L. Ma^{1,63}, L. L. Ma⁵⁰, M. M. Ma^{1,63}, Q. M. Ma¹, R. Q. Ma^{1,63}, R. T. Ma⁶³, X. Y. Ma^{1,58}, Y. Ma^{47,g}, Y. M. Ma³², F. E. Maas¹⁹, M. Maggiora^{74A,74C}, S. Malde⁶⁹, A. Mangoni^{29B}, Y. J. Mao^{47,g}, Z. P. Mao¹, S. Marcello^{74A,74C}, Z. X. Meng⁶⁶, J. G. Messchendorp^{14,64}, G. Mezzadri^{30A}, H. Miao^{1,63}, T. J. Min⁴³, R. E. Mitchell²⁸, X. H. Mo^{1,58,63}, N. Yu. Muchnoi^{13,b}, Y. Nefedov³⁷, F. Nerling^{19,d}, I. B. Nikolaev^{13,b}, Z. Ning^{1,58}, S. Nisar^{11,l}, Y. Niu⁵⁰, S. L. Olsen⁶³, Q. Ouyang^{1,58,63}, S. Pacetti^{29B,29C}, X. Pan⁵⁵, Y. Pan⁵⁷, A. Pathak³⁵, P. Patteri^{29A}, Y. P. Pei^{71,58}, M. Pelizaeus⁴, H. P. Peng^{71,58}, K. Peters^{14,d}, J. L. Ping⁴², R. G. Ping^{1,63}, S. Plura³⁶, S. Pogodin³⁷, V. Prasad⁶⁴, F. Z. Qi¹, H. Qi^{71,58}, H. R. Qi⁶¹, M. Qi⁴³, T. Y. Qi^{12,f}, S. Qian^{1,58}, W. B. Qian⁶³, C. F. Qiao⁶³, J. J. Qin⁷², L. Q. Qin¹⁵, X. P. Qin^{12,f}, X. S. Qin⁵⁰, Z. H. Qin^{1,58}, J. F. Qiu¹, S. Q. Qu⁶¹, C. F. Redmer³⁶, K. J. Ren⁴⁰, A. Rivetti^{74C}, V. Rodin⁶⁴, M. Rolo^{74C}, G. Rong^{1,63}, Ch. Rosner¹⁹, S. N. Ruan⁴⁴, N. Salone⁴⁵, A. Sarantsev^{37,c}, Y. Schelhaas³⁶, K. Schoenning⁷⁵, M. Scodreggio^{30A,30B}, K. Y. Shan^{12,f}, W. Shan²⁵, X. Y. Shan^{71,58}, J. F. Shangguan⁵⁵, L. G. Shao^{1,63}, M. Shao^{71,58}, C. P. Shen^{12,f}, H. F. Shen^{1,63}, W. H. Shen⁶³, X. Y. Shen^{1,63}, B. A. Shi⁶³, H. C. Shi^{71,58}, J. L. Shi¹², J. Y. Shi¹, Q. Q. Shi⁵⁵, R. S. Shi^{1,63}, X. Shi^{1,58}, J. J. Song²⁰, T. Z. Song⁵⁹, W. M. Song^{35,1}, Y. J. Song¹², Y. X. Song^{47,g}, S. Sosio^{74A,74C}, S. Spataro^{74A,74C}, F. Stieler³⁶, Y. J. Su⁶³, G. B. Sun⁷⁶, G. X. Sun¹, H. Sun⁶³, H. K. Sun¹, J. F. Sun²⁰, K. Sun⁶¹, L. Sun⁷⁶, S. S. Sun^{1,63}, T. Sun^{1,63}, W. Y. Sun³⁵, Y. Sun⁹, Y. J. Sun^{71,58}, Y. Z. Sun¹, Z. T. Sun⁵⁰, Y. X. Tan^{71,58}, C. J. Tang⁵⁴, G. Y. Tang¹, J. Tang⁵⁹, Y. A. Tang⁷⁶, L. Y. Tao⁷², Q. T. Tao^{26,h}, M. Tat⁶⁹, J. X. Teng^{71,58}, V. Thoren⁷⁵, W. H. Tian⁵⁹, W. H. Tian⁵², Y. Tian^{32,63}, Z. F. Tian⁷⁶, I. Uman^{62B}, S. J. Wang⁵⁰, B. Wang¹, B. L. Wang⁶³, Bo Wang^{71,58}, C. W. Wang⁴³, D. Y. Wang^{47,g}, F. Wang⁷², H. J. Wang^{39,j,k}, H. P. Wang^{1,63}, J. P. Wang⁵⁰, K. Wang^{1,58}, L. L. Wang¹, M. Wang⁵⁰, Meng Wang^{1,63}, S. Wang^{39,j,k}, S. Wang^{12,f}, T. Wang^{12,f}, T. J. Wang⁴⁴, W. Wang⁵⁹, W. Wang⁷², W. P. Wang^{71,58}, X. Wang^{47,g}, X. F. Wang^{39,j,k}, X. J. Wang⁴⁰, X. L. Wang^{12,f}, Y. Wang⁶¹, Y. D. Wang⁴⁶, Y. F. Wang^{1,58,63}, Y. H. Wang⁴⁸, Y. N. Wang⁴⁶, Y. Q. Wang¹, Yaqian Wang^{18,1}, Yi Wang⁶¹, Z. Wang^{1,58}, Z. L. Wang⁷², Z. Y. Wang^{1,63}, Ziyi Wang⁶³, D. Wei⁷⁰, D. H. Wei¹⁵, F. Weidner⁶⁸, S. P. Wen¹, C. W. Wenzel⁴, U. W. Wiedner⁴, G. Wilkinson⁶⁹, M. Wolke⁷⁵, L. Wollenberg⁴, C. Wu⁴⁰, J. F. Wu^{1,63}, L. H. Wu¹, L. J. Wu^{1,63}, X. Wu^{12,f}, X. H. Wu³⁵, Y. Wu⁷¹, Y. J. Wu³², Z. Wu^{1,58}, L. Xia^{71,58}, X. M. Xian⁴⁰, T. Xiang^{47,g}, D. Xiao^{39,j,k}, G. Y. Xiao⁴³, H. Xiao^{12,f}, S. Y. Xiao¹, Y. L. Xiao^{12,f}, Z. J. Xiao⁴², C. Xie⁴³, X. H. Xie^{47,g}, Y. Xie⁵⁰, Y. G. Xie^{1,58}, Y. H. Xie⁶, Z. P. Xie^{71,58}, T. Y. Xing^{1,63}, C. F. Xu^{1,63}, C. J. Xu⁵⁹, G. F. Xu¹, H. Y. Xu⁶⁶, Q. J. Xu¹⁷, Q. N. Xu³¹, W. Xu^{1,63}, W. L. Xu⁶⁶, X. P. Xu⁵⁵, Y. C. Xu⁷⁸, Z. P. Xu⁴³, Z. S. Xu⁶³, F. Yan^{12,f}, L. Yan^{12,f}, W. B. Yan^{71,58}, W. C. Yan⁸¹, X. Q. Yan¹, H. J. Yang^{51,e}, H. L. Yang³⁵, H. X. Yang¹, Tao Yang¹, Y. Yang^{12,f}, Y. F. Yang⁴⁴, Y. X. Yang^{1,63}, Yifan Yang^{1,63}, Z. W. Yang^{39,j,k}, Z. P. Yao⁵⁰, M. Ye^{1,58}, M. H. Ye⁸, J. H. Yin¹, Z. Y. You⁵⁹, B. X. Yu^{1,58,63}, C. X. Yu⁴⁴, G. Yu^{1,63}, J. S. Yu^{26,h}, T. Yu⁷², X. D. Yu^{47,g}, C. Z. Yuan^{1,63}, L. Yuan², S. C. Yuan¹,

X. Q. Yuan¹, Y. Yuan^{1,63}, Z. Y. Yuan⁵⁹, C. X. Yue⁴⁰, A. A. Zafar⁷³, F. R. Zeng⁵⁰, X. Zeng^{12,f}, Y. Zeng^{26,h}, Y. J. Zeng^{1,63}, X. Y. Zhai³⁵, Y. C. Zhai⁵⁰, Y. H. Zhan⁵⁹, A. Q. Zhang^{1,63}, B. L. Zhang^{1,63}, B. X. Zhang¹, D. H. Zhang⁴⁴, G. Y. Zhang²⁰, H. Zhang⁷¹, H. H. Zhang⁵⁹, H. H. Zhang³⁵, H. Q. Zhang^{1,58,63}, H. Y. Zhang^{1,58}, J. J. Zhang⁵², J. L. Zhang²¹, J. Q. Zhang⁴², J. W. Zhang^{1,58,63}, J. X. Zhang^{39,j,k}, J. Y. Zhang¹, J. Z. Zhang^{1,63}, Jianyu Zhang⁶³, Jiawei Zhang^{1,63}, L. M. Zhang⁶¹, L. Q. Zhang⁵⁹, Lei Zhang⁴³, P. Zhang¹, Q. Y. Zhang^{40,81}, Shuihan Zhang^{1,63}, Shulei Zhang^{26,h}, X. D. Zhang⁴⁶, X. M. Zhang¹, X. Y. Zhang⁵⁰, X. Y. Zhang⁵⁵, Y. Zhang⁶⁹, Y. Zhang⁷², Y. T. Zhang⁸¹, Y. H. Zhang^{1,58}, Yan Zhang^{71,58}, Yao Zhang¹, Z. H. Zhang¹, Z. L. Zhang³⁵, Z. Y. Zhang⁴⁴, Z. Y. Zhang⁷⁶, G. Zhao¹, J. Zhao⁴⁰, J. Y. Zhao^{1,63}, J. Z. Zhao^{1,58}, Lei Zhao^{71,58}, Ling Zhao¹, M. G. Zhao⁴⁴, S. J. Zhao⁸¹, Y. B. Zhao^{1,58}, Y. X. Zhao^{32,63}, Z. G. Zhao^{71,58}, A. Zhemchugov^{37,a}, B. Zheng⁷², J. P. Zheng^{1,58}, W. J. Zheng^{1,63}, Y. H. Zheng⁶³, B. Zhong⁴², X. Zhong⁵⁹, H. Zhou⁵⁰, L. P. Zhou^{1,63}, X. Zhou⁷⁶, X. K. Zhou⁶, X. R. Zhou^{71,58}, X. Y. Zhou⁴⁰, Y. Z. Zhou^{12,f}, J. Zhu⁴⁴, K. Zhu¹, K. J. Zhu^{1,58,63}, L. Zhu³⁵, L. X. Zhu⁶³, S. H. Zhu⁷⁰, S. Q. Zhu⁴³, T. J. Zhu^{12,f}, W. J. Zhu^{12,f}, Y. C. Zhu^{71,58}, Z. A. Zhu^{1,63}, J. H. Zou¹, J. Zu^{71,58}

(BESIII Collaboration)

¹ Institute of High Energy Physics, Beijing 100049, People's Republic of China

² Beihang University, Beijing 100191, People's Republic of China

³ Beijing Institute of Petrochemical Technology, Beijing 102617, People's Republic of China

⁴ Bochum Ruhr-University, D-44780 Bochum, Germany

⁵ Carnegie Mellon University, Pittsburgh, Pennsylvania 15213, USA

⁶ Central China Normal University, Wuhan 430079, People's Republic of China

⁷ Central South University, Changsha 410083, People's Republic of China

⁸ China Center of Advanced Science and Technology, Beijing 100190, People's Republic of China

⁹ China University of Geosciences, Wuhan 430074, People's Republic of China

¹⁰ Chung-Ang University, Seoul, 06974, Republic of Korea

¹¹ COMSATS University Islamabad, Lahore Campus, Defence Road, Off Raiwind Road, 54000 Lahore, Pakistan

¹² Fudan University, Shanghai 200433, People's Republic of China

¹³ G.I. Budker Institute of Nuclear Physics SB RAS (BINP), Novosibirsk 630090, Russia

¹⁴ GSI Helmholtzcentre for Heavy Ion Research GmbH, D-64291 Darmstadt, Germany

¹⁵ Guangxi Normal University, Guilin 541004, People's Republic of China

¹⁶ Guangxi University, Nanning 530004, People's Republic of China

¹⁷ Hangzhou Normal University, Hangzhou 310036, People's Republic of China

¹⁸ Hebei University, Baoding 071002, People's Republic of China

¹⁹ Helmholtz Institute Mainz, Staudinger Weg 18, D-55099 Mainz, Germany

²⁰ Henan Normal University, Xinxiang 453007, People's Republic of China

²¹ Henan University, Kaifeng 475004, People's Republic of China

²² Henan University of Science and Technology, Luoyang 471003, People's Republic of China

²³ Henan University of Technology, Zhengzhou 450001, People's Republic of China

²⁴ Huangshan College, Huangshan 245000, People's Republic of China

²⁵ Hunan Normal University, Changsha 410081, People's Republic of China

²⁶ Hunan University, Changsha 410082, People's Republic of China

²⁷ Indian Institute of Technology Madras, Chennai 600036, India

²⁸ Indiana University, Bloomington, Indiana 47405, USA

²⁹ INFN Laboratori Nazionali di Frascati, (A)INFN Laboratori Nazionali di Frascati, I-00044, Frascati, Italy; (B)INFN

Sezione di Perugia, I-06100, Perugia, Italy; (C)University of Perugia, I-06100, Perugia, Italy

³⁰ INFN Sezione di Ferrara, (A)INFN Sezione di Ferrara, I-44122, Ferrara, Italy; (B)University of Ferrara, I-44122, Ferrara, Italy

³¹ Inner Mongolia University, Hohhot 010021, People's Republic of China

³² Institute of Modern Physics, Lanzhou 730000, People's Republic of China

³³ Institute of Physics and Technology, Peace Avenue 54B, Ulaanbaatar 13330, Mongolia

³⁴ Instituto de Alta Investigación, Universidad de Tarapacá, Casilla 7D, Arica, Chile

³⁵ Jilin University, Changchun 130012, People's Republic of China

³⁶ Johannes Gutenberg University of Mainz, Johann-Joachim-Becher-Weg 45, D-55099 Mainz, Germany

³⁷ Joint Institute for Nuclear Research, 141980 Dubna, Moscow region, Russia

³⁸ Justus-Liebig-Universität Giessen, II. Physikalisches Institut, Heinrich-Buff-Ring 16, D-35392 Giessen, Germany

³⁹ Lanzhou University, Lanzhou 730000, People's Republic of China

⁴⁰ Liaoning Normal University, Dalian 116029, People's Republic of China

⁴¹ Liaoning University, Shenyang 110036, People's Republic of China

⁴² Nanjing Normal University, Nanjing 210023, People's Republic of China

⁴³ Nanjing University, Nanjing 210093, People's Republic of China

⁴⁴ Nankai University, Tianjin 300071, People's Republic of China

⁴⁵ National Centre for Nuclear Research, Warsaw 02-093, Poland

⁴⁶ North China Electric Power University, Beijing 102206, People's Republic of China

⁴⁷ Peking University, Beijing 100871, People's Republic of China

⁴⁸ Qufu Normal University, Qufu 273165, People's Republic of China

- ⁴⁹ Shandong Normal University, Jinan 250014, People's Republic of China
⁵⁰ Shandong University, Jinan 250100, People's Republic of China
⁵¹ Shanghai Jiao Tong University, Shanghai 200240, People's Republic of China
⁵² Shanxi Normal University, Linfen 041004, People's Republic of China
⁵³ Shanxi University, Taiyuan 030006, People's Republic of China
⁵⁴ Sichuan University, Chengdu 610064, People's Republic of China
⁵⁵ Soochow University, Suzhou 215006, People's Republic of China
⁵⁶ South China Normal University, Guangzhou 510006, People's Republic of China
⁵⁷ Southeast University, Nanjing 211100, People's Republic of China
⁵⁸ State Key Laboratory of Particle Detection and Electronics, Beijing 100049, Hefei 230026, People's Republic of China
⁵⁹ Sun Yat-Sen University, Guangzhou 510275, People's Republic of China
⁶⁰ Suranaree University of Technology, University Avenue 111, Nakhon Ratchasima 30000, Thailand
⁶¹ Tsinghua University, Beijing 100084, People's Republic of China
⁶² Turkish Accelerator Center Particle Factory Group, (A)Istinye University, 34010, Istanbul, Turkey; (B)Near East University, Nicosia, North Cyprus, 99138, Mersin 10, Turkey
⁶³ University of Chinese Academy of Sciences, Beijing 100049, People's Republic of China
⁶⁴ University of Groningen, NL-9747 AA Groningen, The Netherlands
⁶⁵ University of Hawaii, Honolulu, Hawaii 96822, USA
⁶⁶ University of Jinan, Jinan 250022, People's Republic of China
⁶⁷ University of Manchester, Oxford Road, Manchester, M13 9PL, United Kingdom
⁶⁸ University of Muenster, Wilhelm-Klemm-Strasse 9, 48149 Muenster, Germany
⁶⁹ University of Oxford, Keble Road, Oxford OX13RH, United Kingdom
⁷⁰ University of Science and Technology Liaoning, Anshan 114051, People's Republic of China
⁷¹ University of Science and Technology of China, Hefei 230026, People's Republic of China
⁷² University of South China, Hengyang 421001, People's Republic of China
⁷³ University of the Punjab, Lahore-54590, Pakistan
⁷⁴ University of Turin and INFN, (A)University of Turin, I-10125, Turin, Italy; (B)University of Eastern Piedmont, I-15121, Alessandria, Italy; (C)INFN, I-10125, Turin, Italy
⁷⁵ Uppsala University, Box 516, SE-75120 Uppsala, Sweden
⁷⁶ Wuhan University, Wuhan 430072, People's Republic of China
⁷⁷ Xinyang Normal University, Xinyang 464000, People's Republic of China
⁷⁸ Yantai University, Yantai 264005, People's Republic of China
⁷⁹ Yunnan University, Kunming 650500, People's Republic of China
⁸⁰ Zhejiang University, Hangzhou 310027, People's Republic of China
⁸¹ Zhengzhou University, Zhengzhou 450001, People's Republic of China
- ^a Also at the Moscow Institute of Physics and Technology, Moscow 141700, Russia
^b Also at the Novosibirsk State University, Novosibirsk, 630090, Russia
^c Also at the NRC "Kurchatov Institute", PNPI, 188300, Gatchina, Russia
^d Also at Goethe University Frankfurt, 60323 Frankfurt am Main, Germany
^e Also at Key Laboratory for Particle Physics, Astrophysics and Cosmology, Ministry of Education; Shanghai Key Laboratory for Particle Physics and Cosmology; Institute of Nuclear and Particle Physics, Shanghai 200240, People's Republic of China
^f Also at Key Laboratory of Nuclear Physics and Ion-beam Application (MOE) and Institute of Modern Physics, Fudan University, Shanghai 200443, People's Republic of China
^g Also at State Key Laboratory of Nuclear Physics and Technology, Peking University, Beijing 100871, People's Republic of China
^h Also at School of Physics and Electronics, Hunan University, Changsha 410082, China
ⁱ Also at Guangdong Provincial Key Laboratory of Nuclear Science, Institute of Quantum Matter, South China Normal University, Guangzhou 510006, China
^j Also at Frontiers Science Center for Rare Isotopes, Lanzhou University, Lanzhou 730000, People's Republic of China
^k Also at Lanzhou Center for Theoretical Physics, Lanzhou University, Lanzhou 730000, People's Republic of China
^l Also at the Department of Mathematical Sciences, IBA, Karachi 75270, Pakistan

The quantum entangled $J/\psi \rightarrow \Sigma^+ \bar{\Sigma}^-$ pairs from $(1.0087 \pm 0.0044) \times 10^{10}$ J/ψ events taken by the BESIII detector are used to study the non-leptonic two-body weak decays $\Sigma^+ \rightarrow n\pi^+$ and $\bar{\Sigma}^- \rightarrow \bar{n}\pi^-$. The CP -odd weak decay parameters of the decays $\Sigma^+ \rightarrow n\pi^+$ (α_+) and $\bar{\Sigma}^- \rightarrow \bar{n}\pi^-$ ($\bar{\alpha}_-$) are determined to be $-0.0565 \pm 0.0047_{\text{stat}} \pm 0.0022_{\text{syst}}$ and $0.0481 \pm 0.0031_{\text{stat}} \pm 0.0019_{\text{syst}}$, respectively. The decay parameter $\bar{\alpha}_-$ is measured for the first time, and the accuracy of α_+ is improved by a factor of four compared to the previous results. The simultaneously determined decay parameters allow the first precision CP symmetry test for any hyperon decay with a neutron in the final state with the measurement of $A_{CP} = (\alpha_+ + \bar{\alpha}_-)/(\alpha_+ - \bar{\alpha}_-) = -0.080 \pm 0.052_{\text{stat}} \pm 0.028_{\text{syst}}$. Assuming CP conservation, the average decay parameter is determined as $\langle \alpha_+ \rangle = (\alpha_+ - \bar{\alpha}_-)/2 = -0.0506 \pm 0.0026_{\text{stat}} \pm 0.0019_{\text{syst}}$, while the ratios α_+/α_0 and $\bar{\alpha}_-/\bar{\alpha}_0$ are $-0.0490 \pm 0.0032_{\text{stat}} \pm 0.0021_{\text{syst}}$ and

$-0.0571 \pm 0.0053_{\text{stat}} \pm 0.0032_{\text{sys}}$, where α_0 and $\bar{\alpha}_0$ are the decay parameters of the decays $\Sigma^+ \rightarrow p\pi^0$ and $\bar{\Sigma}^- \rightarrow \bar{p}\pi^0$, respectively.

Charge-parity (CP) violation is one of Sakharov's three essential conditions for understanding the matter-antimatter asymmetry in the universe [1]. Despite the established presence of CP violation in the decays of K , B , and D mesons [2–7], the standard model (SM) of particle physics, as described by the Kobayashi-Maskawa mechanism, is insufficient in fully explaining the preponderance of matter over antimatter in the universe [8]. As a result, it is imperative to continue searching for new sources of CP violation, particularly in the hyperon sector [9]. The non-leptonic decays of spin-1/2 hyperons are suitable for CP violation studies. In such decays, the decay asymmetry parameters α , β and γ are defined in terms of the S -wave (parity violating) and P -wave (parity conserving) amplitudes [10]:

$$\alpha = \frac{2\text{Re}(S^*P)}{|S|^2 + |P|^2}, \beta = \frac{2\text{Im}(S^*P)}{|S|^2 + |P|^2}, \gamma = \frac{|S|^2 - |P|^2}{|S|^2 + |P|^2}.$$

Only two of these asymmetry parameters are independent. The magnitude of polarization of spin-1/2 hyperons can be inferred in two-body weak decays due to their self-analyzing nature. The polar angle distribution of the daughter nucleons is given by $dN/d\Omega = \frac{1}{4\pi}(1 + \alpha\mathbf{P} \cdot \hat{\mathbf{p}})$. Here, \mathbf{P} is the hyperon polarization vector, and $\hat{\mathbf{p}}$ is the unit vector along the nucleon momentum in the hyperon rest frame. Correspondingly, the decay asymmetry parameter of the anti-hyperon is denoted as $\bar{\alpha}$. Because α and $\bar{\alpha}$ are CP -odd, $A_{CP} = (\alpha + \bar{\alpha})/(\alpha - \bar{\alpha})$ can be used to test CP conservation [11, 12]. A non-zero value of A_{CP} would indicate CP violation.

Theoretically, there are two predictions for CP violation in non-leptonic two-body weak decays of Σ . In the seminal work by Donoghue et al., the CP violation contribution in $\Sigma^+ \rightarrow n\pi^+$ was predicted to be -1.6×10^{-4} [13]. The most recent study by Tandean and Valencia used heavy baryon Chiral perturbation theory and predicted the CP violation of $\Sigma^+ \rightarrow n\pi^+$ to be 3.9×10^{-4} . Although the above two predictions are at the same level, Ref. [13] does not consider the P -wave factorization contribution, which can change the prediction by a factor of ten. To determine the SM CP violation contribution, the experimentally determined asymmetry parameters are used as part of the input. Due to the large experimental uncertainty of the $\Sigma^+ \rightarrow n\pi^+$ asymmetry parameter α_+ , the uncertainties in the CP violation estimations of $\Sigma^+ \rightarrow n\pi^+$ are greater than those of other hyperons, and the predicted CP violation is an order of magnitude greater than those of $\Sigma^+ \rightarrow p\pi^0$, $\Sigma^- \rightarrow n\pi^-$ and $\Lambda \rightarrow p\pi^-$ [14].

Recently it was pointed out that the experimental value of the decay asymmetry α_0 for $\Sigma^+ \rightarrow p\pi^0$ is not consistent with the $\Delta I = 1/2$ rule [15], where ΔI refers to

the isospin difference between the initial and final states. Therefore, a precision measurement of the decay asymmetry α_+ for $\Sigma^+ \rightarrow n\pi^+$ is needed to determine the contributions of the $\Delta I = 3/2$ and $\Delta I = 1/2$ weak transitions to Σ decays [16].

Experimentally, the decay asymmetry parameters α_0 and its charge-conjugated (c.c.) equivalent $\bar{\alpha}_0$ have been well measured [17]. For the decay of $\Sigma^+ \rightarrow n\pi^+$, there are only two measurements of α_+ from fixed-target experiments, performed more than fifty years ago. Although the two existing results 0.069 ± 0.017 [18] and 0.037 ± 0.049 [19] are in agreement with each other, they are relatively imprecise compared with α_0 and also compatible with zero. Furthermore, the corresponding decay parameter $\bar{\alpha}_-$ of $\bar{\Sigma}^- \rightarrow \bar{n}\pi^-$ has never been measured before. Precision measurements of the decay parameters of $\Sigma^+ \rightarrow n\pi^+ + \text{c.c.}$ would provide a first precision test of CP symmetry in hyperon to neutron decays and supply important experimental input to sharpen CP violation predictions of all non-leptonic two-body weak decays of Σ . However, the relatively small α_+ and $\bar{\alpha}_-$ values, the Σ polarization value determination, and the difficulties in neutron and anti-neutron detection all represent a challenge for an accurate experimental measurement.

The BESIII experiment provides a unique environment to study both hyperon production and decay properties in electron-positron annihilation to $\Sigma^+\bar{\Sigma}^-$ pairs via the intermediate J/ψ resonance, where the above challenges can be well addressed. In this entangled quantum system, the decay parameters of Σ^+ and $\bar{\Sigma}^-$ are correlated, allowing for a precise determination of the asymmetry parameters and the CP symmetry. The $e^+e^- \rightarrow J/\psi \rightarrow \Sigma^+\bar{\Sigma}^-$ process is described by the Ψ electric and magnetic form factors, G_E^Ψ and G_M^Ψ [20]. These two Ψ form factors are formally equivalent to the Σ electric and magnetic form factors [21–25]. They are usually parameterized by two real parameters $\alpha_{J/\psi}$ and $\Delta\Phi$, which correspond to the angular decay asymmetry and the relative phase between the two form factors, respectively. The observable $\Delta\Phi$ is related to the spin-polarization of the produced $\Sigma^+\bar{\Sigma}^-$ pair. The Σ polarization is perpendicular to the production plane and depends on the opening angle θ_{Σ^+} between the Σ^+ and electron (e^-) beam in the reaction center-of-mass frame, as shown in Fig. 1. The first polarization measurement of $J/\psi \rightarrow \Sigma^+\bar{\Sigma}^-$ was reported by the BESIII collaboration with $\Sigma^+ \rightarrow p\pi^0$ and $\bar{\Sigma}^- \rightarrow \bar{p}\pi^0$ based on 1.3 billion J/ψ events [26]. The significant polarization provides the prerequisite for α_+ and $\bar{\alpha}_-$ measurements.

The production and decay process $e^+e^- \rightarrow J/\psi \rightarrow \Sigma^+(\rightarrow N\pi)\bar{\Sigma}^-(\rightarrow \bar{N}\pi)$ is described with five observables $\xi = (\theta_{\Sigma^+}, \theta_N, \phi_N, \theta_{\bar{N}}, \phi_{\bar{N}})$ [20]. Here θ_N, ϕ_N and $\theta_{\bar{N}}, \phi_{\bar{N}}$

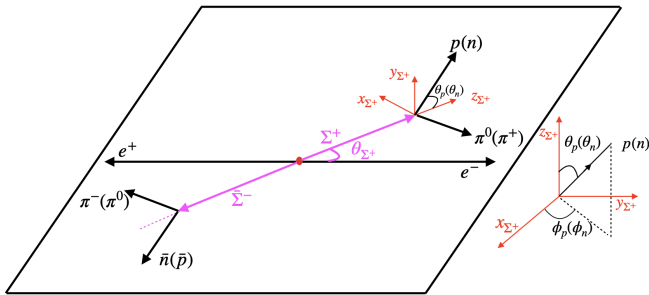


Figure 1. The helicity frame definitions for $J/\psi \rightarrow \Sigma^+\bar{\Sigma}^-, \Sigma^+ \rightarrow p\pi^0(n\pi^+)$, $\bar{\Sigma}^- \rightarrow \bar{n}\pi^-(\bar{p}\pi^0)$. In the e^+e^- center-of-mass system, θ_{Σ} is the angle between the Σ^+ and the electron beam direction. The z_{Σ^+} axis is the moving direction of Σ^+ in the J/ψ rest frame, the y_{Σ^+} axis is perpendicular to the plane of Σ^+ and electron, and the x_{Σ^+} axis is defined by the right-handed coordinate system.

are the polar and azimuthal angles of the nucleon and anti-nucleon measured in the rest frames of their respective mother particles. The differential cross section $\mathcal{W}(\xi)$ is defined as

$$\begin{aligned} \mathcal{W}(\xi) = & \mathcal{T}_0(\xi) + \alpha_{J/\psi} \mathcal{T}_5(\xi) \\ & + \alpha\bar{\alpha} \left(\mathcal{T}_1(\xi) + \sqrt{1 - \alpha_{J/\psi}^2} \cos(\Delta\Phi) \mathcal{T}_2(\xi) + \alpha_{J/\psi} \mathcal{T}_6(\xi) \right) \\ & + \sqrt{1 - \alpha_{J/\psi}^2} \sin(\Delta\Phi) (\alpha \mathcal{T}_3(\xi) + \bar{\alpha} \mathcal{T}_4(\xi)), \end{aligned}$$

where \mathcal{T}_i , ($i = 0, 1 \dots 6$) are angular functions dependent on ξ and described in detail in Ref. [20]. According to the above cross-section formula, if the process of $J/\psi \rightarrow \Sigma^+\bar{\Sigma}^-$ with $\Sigma^+ \rightarrow n\pi^+$, $\bar{\Sigma}^- \rightarrow \bar{n}\pi^-$ is used with the α and $\bar{\alpha}$ parameters close to zero, the cross section will be small, and the determination of the parameters imprecise. Moreover, the simultaneous detection of both the neutron and anti-neutron will be difficult. In addition, the process of $J/\psi \rightarrow \Sigma^-\bar{\Sigma}^+$ with $\Sigma^- \rightarrow n\pi^-$, $\bar{\Sigma}^+ \rightarrow \bar{n}\pi^+$ with the same final state could contaminate our signal. To overcome these disadvantages, we instead use $J/\psi \rightarrow \Sigma^+\bar{\Sigma}^-$ with $\Sigma^+ \rightarrow p\pi^0(n\pi^+)$ and $\bar{\Sigma}^- \rightarrow \bar{n}\pi^-(\bar{p}\pi^0)$. Benefiting from the large decay parameters $\alpha_0 = -0.998 \pm 0.037_{\text{stat}} \pm 0.009_{\text{syst}}$ and $\bar{\alpha}_0 = 0.990 \pm 0.037_{\text{stat}} \pm 0.011_{\text{syst}}$ [26], the measurement accuracy can be improved by 17.4 times compared with the neutron anti-neutron final state. Also, since Σ^- cannot decay to $\bar{p}\pi^0$, the $J/\psi \rightarrow \Sigma^-\bar{\Sigma}^+$ background is highly suppressed.

This Letter is based on a data sample of $(1.0087 \pm 0.0044) \times 10^{10}$ J/ψ events [27] taken with the BESIII detector operating at the BEPCII collider. Details about the design and performance of the BESIII detector are given in Ref. [28]. Candidate events for the process $J/\psi \rightarrow \Sigma^+\bar{\Sigma}^-$ with subsequent $\Sigma^+ \rightarrow p\pi^0(n\pi^+)$ and $\bar{\Sigma}^- \rightarrow \bar{n}\pi^-(\bar{p}\pi^0)$ decays must have two charged tracks with opposite charges and at least two photons. Charged

tracks detected in the multi-layer drift chamber (MDC) are required to be within a polar angle (θ) range of $|\cos\theta| < 0.93$, where θ is defined with respect to the z axis, the symmetry axis of the MDC. For each track, the distance of the closest approach to the interaction point must be less than 10 cm along the z axis, and less than 2 cm in the transverse plane.

The particle identification (PID) system identifies the two candidate charged tracks as $p\pi^-$ or $\bar{p}\pi^+$ based on the measured energy loss in the MDC and the flight time in the time-of-flight system. Each track is assigned to the particle type corresponding to the hypothesis with the highest confidence level.

Photon candidates are identified using showers in the electromagnetic calorimeter (EMC). The deposited energy of each shower must be more than 25 MeV in the barrel region ($|\cos\theta| < 0.80$) and more than 50 MeV in the end-cap region ($0.86 < |\cos\theta| < 0.92$). To exclude showers that originate from charged tracks, the opening angle subtended by the EMC shower and the position of the closest charged track at the EMC must be greater than 10° as measured from the interaction point. To suppress electronic noise and showers unrelated to the event, the difference between the EMC time and the event start time is required to be within $[0, 700]$ ns.

Candidates for π^0 are selected as photon pairs with an invariant mass in the interval of $(m_{\pi^0} - 60 \text{ MeV}/c^2) < M_{\gamma\gamma} < (m_{\pi^0} + 40 \text{ MeV}/c^2)$, where m_{π^0} is the known π^0 mass [17]. In addition, a one-constraint (1C) kinematic fit is performed on the selected photon pairs, constraining the invariant mass to the known π^0 mass. The χ^2_{1C} of the kinematic fit is required to be less than 25. At least one candidate π^0 is required.

To select $J/\psi \rightarrow \Sigma^+\bar{\Sigma}^-$ with $\Sigma^+ \rightarrow p\pi^0$ and $\bar{\Sigma}^- \rightarrow \bar{n}\pi^-$, the anti-neutron energy deposition in the EMC is required to be at least 0.5 GeV. The second moment, defined as $\sum_i E_i r_i^2 / \sum_i E_i$, is required to be greater than 20. Here E_i is the energy deposition in the i_{th} crystal and r_i is the radial distance of the i_{th} crystal from the cluster center. The opening angle $\theta_{\gamma, \bar{n}}$ between photon candidates and the \bar{n} track is required to be greater than 20° . For this process, a four-constraint (4C) kinematic fit is applied by imposing energy-momentum conservation and an additional π^0 mass constraint, where the direction of the \bar{n} is measured and the energy is unmeasured. A two-constraint (2C) kinematic fit is applied to the $J/\psi \rightarrow \Sigma^+\bar{\Sigma}^-$ process, with $\Sigma^+ \rightarrow n\pi^+$ and $\bar{\Sigma}^- \rightarrow \bar{p}\pi^0$. Energy-momentum conservation and an additional π^0 mass constraint are imposed in this fit, with the neutron being treated as a missing particle. The 4C and 2C kinematic fit chi-squares, χ^2_{4C} and χ^2_{2C} , are both required to be less than 100. If the number of π^0 candidates in an event is more than one, the combination with the minimum χ^2_{4C} or χ^2_{2C} is selected as the final candidate.

To investigate possible background after applying the

event selection criteria, an inclusive Monte Carlo (MC) sample of 10 billion J/ψ events has been examined with TopoAna [29]. All particle decays are modeled with EVTGEN [30] using branching fractions either taken from the Particle Data Group (PDG) [17], when available, or otherwise estimated with LUNDCHARM [31]. The main peaking backgrounds are $J/\psi \rightarrow \gamma \Sigma^+ \bar{\Sigma}^-$ and $J/\psi \rightarrow \gamma \eta_c, \eta_c \rightarrow \Sigma^+ \bar{\Sigma}^-$, which both contribute 0.2% of the signal strength and are negligible. The non-peaking background mainly includes $J/\psi \rightarrow \Delta^+ \bar{\Delta}^- \rightarrow p\pi^0 \bar{n}\pi^- (n\pi^+ \bar{p}\pi^0)$ and $J/\psi \rightarrow p\pi^0 \bar{n}\pi^- (n\pi^+ \bar{p}\pi^0)$ whose contributions are estimated to be 1.4% and 1.6% with a two-dimensional sideband method. Figure 2 shows the distributions of $M_{\bar{n}\pi^-}$ versus $M_{p\pi^0}$ and $M_{n\pi^+}$ versus $M_{\bar{p}\pi^0}$ for the two decay modes. The signal regions in the red rectangles are defined as: $1.17 < M_{p\pi^0} (M_{\bar{p}\pi^0}) < 1.20$ GeV/ c^2 and $1.18 < M_{\bar{n}\pi^-} (M_{n\pi^+}) < 1.20$ GeV/ c^2 . To estimate the non-peaking background contributions, four sideband regions have been selected, denoted as green rectangles in the plots. Each sideband region has the same area as the signal region and is placed at a distance of about 2σ from the signal boundary, where σ is the invariant mass resolution of Σ^+ and $\bar{\Sigma}^-$. The background events are estimated using $f \times \sum_{i=1}^4 B_i$, where B_i is the number of events in the i_{th} sideband region, and the scale factor f is defined as the background ratio between the signal and sideband regions. Using a two-dimensional fit on the distribution of $M_{p\pi^0}$ versus $M_{\bar{n}\pi^-}$ or $M_{n\pi^+}$ versus $M_{\bar{p}\pi^0}$, the scale factors are determined to be 0.265 ± 0.001 and 0.259 ± 0.001 for these two decay channels, respectively. Here the uncertainties are statistical only.

An unbinned maximum likelihood fit is performed in the five angular dimensions ξ [26] simultaneously on the two datasets to determine the parameters $\{\alpha_{J/\psi}, \Delta\Phi_{J/\psi}, \alpha_+, \bar{\alpha}_-\}$. Following the approach in Ref. [32], the multidimensional fit takes the reconstruction efficiency into account in a model-independent way and background contribution has been considered according to the scale factors f . The numerical fit results are summarized in Table I. The relative phase between the Ψ electric and magnetic form factors is determined to be $\Delta\Phi_{J/\psi} = (-0.2772 \pm 0.0044_{\text{stat}} \pm 0.0041_{\text{sys}})$ rad, which implies Σ spin polarization is observed. The moment related to the polarization is defined as

$$M(\cos \theta_{\Sigma^+}) = \frac{m}{n} \sum_i^{n_k} (\sin \theta_N^k \sin \phi_N^k - \sin \theta_N^k \sin \phi_N^k).$$

Here, $m = 40$ is the number of bins, n is the total number of events in the data sample, and n_k is the number of events in the k_{th} $\cos \theta_{\Sigma^+}$ bin. The expected angular dependence of the moment is $\frac{dM}{d \cos \theta_{\Sigma^+}} \sim \sqrt{1 - \alpha_{J/\psi}^2} \alpha_+ \sin \Delta\Phi_{J/\psi} \cos \theta_{\Sigma^+} \sin \theta_{\Sigma^+}$. In Fig. 3, the black points represent data and follow the expectation as shown by the red line. As $\Delta\Phi_{J/\psi}$ is not zero, it

is possible to determine the asymmetry parameters α_+ and $\bar{\alpha}_-$ simultaneously. The asymmetry decay parameter α_+ is measured to be $0.0481 \pm 0.0031_{\text{stat}} \pm 0.0019_{\text{sys}}$, with a precision improved by a factor of 4.7 compared to the previous best measurement [18]. The asymmetry decay parameter $\bar{\alpha}_-$ is determined for the first time as $-0.0565 \pm 0.0047_{\text{stat}} \pm 0.0022_{\text{sys}}$. Assuming no CP violation, the average decay asymmetry is calculated to be $\langle \alpha_+ \rangle = (\alpha_+ - \bar{\alpha}_-)/2 = 0.0506 \pm 0.0026_{\text{stat}} \pm 0.0019_{\text{sys}}$.

Table I. The decay parameters of $J/\psi \rightarrow \Sigma^+ \bar{\Sigma}^-, \Sigma^+ \rightarrow p\pi^0 (n\pi^+), \bar{\Sigma}^- \rightarrow \bar{n}\pi^- (\bar{p}\pi^0)$. The first uncertainties are statistical and the second systematic. Dash (-) represents no experimental measurement.

Parameter	This work	Previous result
$\alpha_{J/\psi}$	$-0.5156 \pm 0.0030 \pm 0.0061$	$-0.508 \pm 0.006 \pm 0.004$ [26]
$\Delta\Phi_{J/\psi}$ (rad)	$-0.2772 \pm 0.0044 \pm 0.0041$	$-0.270 \pm 0.012 \pm 0.009$ [26]
α_+	$0.0481 \pm 0.0031 \pm 0.0019$	0.069 ± 0.017 [18]
$\bar{\alpha}_-$	$-0.0565 \pm 0.0047 \pm 0.0022$	-
α_+/α_0	$-0.0490 \pm 0.0032 \pm 0.0021$	-0.069 ± 0.021 [33]
$\bar{\alpha}_-/\bar{\alpha}_0$	$-0.0571 \pm 0.0053 \pm 0.0032$	-
A_{CP}	$-0.080 \pm 0.052 \pm 0.028$	-
$\langle \alpha_+ \rangle$	$0.0506 \pm 0.0026 \pm 0.0019$	-

Table II. The absolute systematic uncertainties in $\alpha_{J/\psi}$, $\Delta\Phi_{J/\psi}$, $\bar{\alpha}_-$ and α_+ .

Source	$\alpha_{J/\psi}$	$\Delta\Phi_{J/\psi}$	$\bar{\alpha}_-$	α_+
MC efficiency correction	0.0059	0.0005	0.0016	0.0011
Kinematic fit	0.0003	0.0004	0.0007	0.0003
Signal mass window	0.0015	0.0021	0.0010	0.0009
Background	0.0001	0.0007	0.0003	0.0002
Fitting method	0.0007	0.0028	0.0007	0.0012
Decay parameters	0.0000	0.0020	0.0003	0.0003
Total	0.0061	0.0041	0.0022	0.0019

The systematic uncertainties are listed in Table II, which is divided into two categories. The first category is from the event selection, including the uncertainties for MDC tracking, PID, π^0 and \bar{n} reconstructions, kinematic fit, background estimations, as well as the Σ^+ and $\bar{\Sigma}^-$ mass window requirements. The second category includes the uncertainties associated with the fit procedure. The individual uncertainties are assumed to be uncorrelated and are therefore added in quadrature. The uncertainties due to potential efficiency differences between data and simulation for charged-particle tracking and PID have been investigated with a $J/\psi \rightarrow p\bar{p}\pi^+\pi^-$ control sample, and those due to neutral π^0 and \bar{n} reconstructions are estimated from $J/\psi \rightarrow \Sigma^+ (p\pi^0) \bar{\Sigma}^- (\bar{p}\pi^0)$ and $J/\psi \rightarrow p\bar{n}\pi^-$ control samples. Using these control samples, we determine the correction factors and apply them in the MC simulation to obtain the nominal results. The uncertainty of the correction factors is estimated by changing them within 1σ regions. The differences to the nominal results are taken as the MC efficiency correction systematic uncertainties. The systematic uncertainties

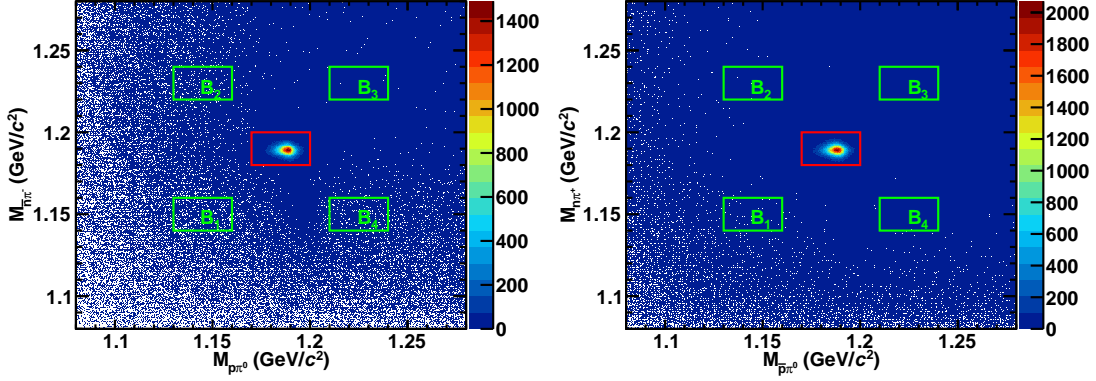


Figure 2. Distributions of (left) $M_{\bar{n}\pi^-}$ versus $M_{p\pi^0}$ for $J/\psi \rightarrow \Sigma^+\bar{\Sigma}^-$ with $\Sigma^+ \rightarrow p\pi^0, \bar{\Sigma}^- \rightarrow \bar{n}\pi^-$, and (right) $M_{n\pi^+}$ versus $M_{\bar{p}\pi^0}$ for $J/\psi \rightarrow \Sigma^+\bar{\Sigma}^-$ with $\Sigma^+ \rightarrow n\pi^+, \bar{\Sigma}^- \rightarrow \bar{p}\pi^0$. The red boxes denote the signal regions and the green ones indicate the sideband regions.

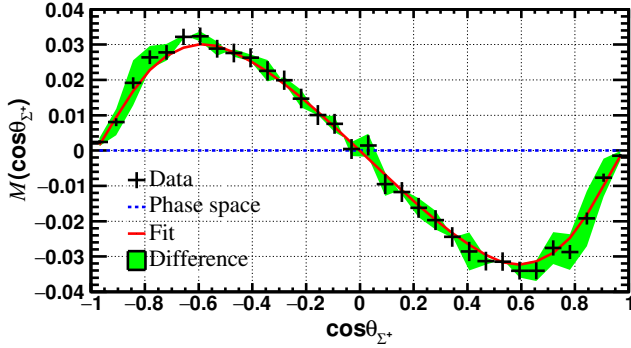


Figure 3. The moment $M(\cos\theta_{\Sigma^+})$ for data, that is not corrected for acceptance and reconstruction efficiency, as a function of $\cos\theta_{\Sigma^+}$ for $J/\psi \rightarrow \Sigma^+\bar{\Sigma}^-$ with the two decay channels: $\Sigma^+ \rightarrow p\pi^0, \bar{\Sigma}^- \rightarrow \bar{n}\pi^-$ and $\Sigma^+ \rightarrow n\pi^+, \bar{\Sigma}^- \rightarrow \bar{p}\pi^0$. The black points with error bars are data with background subtracted, the red solid line is the fit result and the blue dashed line represents the distribution without polarization uniformly distributed in phase space. The height of green band shows the absolute difference between the two decay channels with background subtracted.

due to the kinematic fits are examined by comparing the detection efficiencies with and without helix parameter corrections, which are used to reduce the discrepancies between data and MC simulation [34]. The differences in detection efficiencies with and without corrections are assigned as the systematic uncertainties. To estimate the systematic uncertainty associated with the signal mass window, the window is changed by 3σ (± 5 MeV), where σ is the invariant mass resolution of Σ^+ and $\bar{\Sigma}^-$. The fits are repeated using the new mass window, and the differences of results to the nominal values are regarded as the corresponding systematic uncertainties. The systematic uncertainty caused by the background estimation is studied by varying the length and width of four side-

band boxes within ± 5 MeV. The largest differences in the parameters are taken as the systematic uncertainties. To validate the reliability of the fit results, a set of 100 pseudo-data samples are simulated and subjected to the same selection criteria. In these samples, the differential cross section is based on the decay parameters listed in Table I. The systematic uncertainties from the fit approach are assumed to be the deviations between the inputs and average outputs. In the nominal fit, the parameters of α_0 and $\bar{\alpha}_0$ are fixed at the world average values [17]. By changing the parameter within $\pm 1\sigma$ (0.006) regions for α_0 and $\bar{\alpha}_0$, the changes between the new and nominal fit results are taken as systematic uncertainties.

In summary, based on a data sample of $(1.0087 \pm 0.0044) \times 10^{10}$ J/ψ events collected at the BESIII detector, the five-dimensional angular analysis of the processes of $J/\psi \rightarrow \Sigma^+\bar{\Sigma}^-$ ($\Sigma^+ \rightarrow p\pi^0, \bar{\Sigma}^- \rightarrow \bar{n}\pi^-$ and $\Sigma^+ \rightarrow n\pi^+, \bar{\Sigma}^- \rightarrow \bar{p}\pi^0$) is performed. The decay parameters $\alpha_{J/\psi}$ and $\Delta\Phi_{J/\psi}$ are measured to be $-0.5156 \pm 0.0030_{\text{stat}} \pm 0.0061_{\text{syst}}$ and $(-0.2772 \pm 0.0044_{\text{stat}} \pm 0.0041_{\text{syst}})$ rad, respectively, which are consistent with the previous measurements but with improved precision [26]. The nonzero value of $\Delta\Phi_{J/\psi}$ in the $J/\psi \rightarrow \Sigma^+\bar{\Sigma}^-$ decay, which implies the existence of polarization, is confirmed with two different Σ decay channels, $J/\psi \rightarrow \Sigma^+\bar{\Sigma}^- \rightarrow p\pi^0\bar{n}\pi^-$ ($n\pi^+\bar{p}\pi^0$) and $J/\psi \rightarrow \Sigma^+\bar{\Sigma}^- \rightarrow p\pi^0\bar{p}\pi^0$. Therefore, the decay asymmetry parameters α_+ and $\bar{\alpha}_-$ are determined simultaneously. The parameters α_+ and α_+/α_0 determined in this work are consistent with the PDG averages but with significantly improved precision, and $\bar{\alpha}_-$ and $\bar{\alpha}_-/\bar{\alpha}_0$ are measured for the first time. The average decay asymmetry parameter is $0.0506 \pm 0.0026_{\text{stat}} \pm 0.0019_{\text{syst}}$, which differs from zero by 16σ . In contrast, the previous best measurement only deviates from zero by about 3σ [18]. This result is crucial to test the $|\Delta I| = 1/2$ rule and

study the high order isospin transitions [33]. Our precise measurement of the decay asymmetry parameter in the neutron mode is of vital importance to the CP violation prediction [14]. This is the first study to test CP symmetry in the hyperon to neutron decay, and the result is consistent with CP -conservation.

The BESIII Collaboration thanks the staff of BEPCII and the IHEP computing center for their strong support. This work is supported in part by National Key R&D Program of China under Contracts Nos. 2020YFA0406300, 2020YFA0406400; National Natural Science Foundation of China (NSFC) under Contracts Nos. 11635010, 11735014, 11835012, 11935015, 11935016, 11935018, 11961141012, 12022510, 12025502, 12035009, 12035013, 12061131003, 12192260, 12192261, 12192262, 12192263, 12192264, 12192265, 12221005, 12225509, 12235017; the Chinese Academy of Sciences (CAS) Large-Scale Scientific Facility Program; the CAS Center for Excellence in Particle Physics (CCEPP); CAS Key Research Program of Frontier Sciences under Contracts Nos. QYZDJ-SSW-SLH003, QYZDJ-SSW-SLH040; 100 Talents Program of CAS; The Institute of Nuclear and Particle Physics (INPAC) and Shanghai Key Laboratory for Particle Physics and Cosmology; Sponsored by Shanghai Pujiang Program(20PJ1401700); ERC under Contract No. 758462; European Union's Horizon 2020 research and innovation programme under Marie Skłodowska-Curie grant agreement under Contract No. 894790; German Research Foundation DFG under Contracts Nos. 443159800, 455635585, Collaborative Research Center CRC 1044, FOR5327, GRK 2149; Istituto Nazionale di Fisica Nucleare, Italy; Ministry of Development of Turkey under Contract No. DPT2006K-120470; National Research Foundation of Korea under Contract No. NRF-2022R1A2C1092335; National Science and Technology fund of Mongolia; National Science Research and Innovation Fund (NSRF) via the Program Management Unit for Human Resources & Institutional Development, Research and Innovation of Thailand under Contract No. B16F640076; Polish National Science Centre under Contract No. 2019/35/O/ST2/02907; The Swedish Research Council; the Olle Engkvist Foundation under contract no. 200-0605; U. S. Department of Energy under Contract No. DE-FG02-05ER41374.

-
- [1] A. D. Sakharov, *Pisma Zh. Eksp. Teor. Fiz.* **5**, 32 (1967).
 [2] J. H. Christenson, J. W. Cronin, V. L. Fitch and R. Turlay, *Phys. Rev. Lett.* **13**, 138 (1964).
 [3] A. Abashian *et al.* (Belle Collaboration), *Phys. Rev. Lett.* **86**, 2509 (2001).

- [4] B. Aubert *et al.* (BaBar Collaboration), *Phys. Rev. Lett.* **86**, 2515 (2001).
 [5] Y. Chao *et al.* (Belle Collaboration), *Phys. Rev. Lett.* **93**, 191802 (2004).
 [6] B. Aubert *et al.* (BaBar Collaboration), *Phys. Rev. Lett.* **93**, 131801 (2004).
 [7] R. Aaij *et al.* (LHCb Collaboration), *Phys. Rev. Lett.* **122**, 211803 (2019).
 [8] M. E. Peskin, *Nature* **419**, 24 (2002).
 [9] I. I. Bigi, X. W. Kang and H. B. Li, *Chin. Phys. C* **42**, 013101 (2018); M. Ablikim *et al.* (BESIII Collaboration), *Chin. Phys. C* **44**, 040001 (2020).
 [10] T. D. Lee and C. N. Yang, *Phys. Rev.* **108**, 1645-1647 (1957).
 [11] S. Okubo, *Phys. Rev.* **109**, 984 (1958).
 [12] A. Pais, *Phys. Rev. Lett.* **3**, 242 (1959).
 [13] J. F. Donoghue, X. G. He and S. Pakvasa, *Phys. Rev. D* **34**, 833 (1986).
 [14] J. Tandean and G. Valencia, *Phys. Rev. D* **67**, 056001 (2003).
 [15] N. Salone, P. Adlarson, V. Batozskaya, A. Kupsc, S. Leupold and J. Tandean, *Phys. Rev. D* **105**, 116022 (2022).
 [16] O. E. Overseth and S. Pakvasa, *Phys. Rev.* **184**, 1663 (1969).
 [17] R. L. Workman *et al.* (Particle Data Group), *PTEP* **2022**, 083C01 (2022).
 [18] R. O. Bangerter, <https://www.osti.gov/biblio/4750337>.
 [19] D. Berley, S. P. Yamin, S. S. Hertzbach, R. R. Kofler, G. W. Meisner, J. Button-Shafer, S. S. Yamamoto, W. Heintzelman, M. Schiff, and J. Thompson and W. Willis, *Phys. Rev. D* **1**, 2015 (1970).
 [20] G. Fäldt and A. Kupsc, *Phys. Lett. B* **772**, 16 (2017).
 [21] A. Z. Dubnickova, S. Dubnicka and M. P. Rekaló, *Nuovo Cim. A* **109**, 241 (1996).
 [22] G. I. Gakh and E. Tomasi-Gustafsson, *Nucl. Phys. A* **771**, 169 (2006).
 [23] H. Czyz, A. Grzelinska and J. H. Kuhn, *Phys. Rev. D* **75**, 074026 (2007).
 [24] G. Fäldt, *Eur. Phys. J. A* **51**, 74 (2015).
 [25] G. Fäldt, *Eur. Phys. J. A* **52**, 141 (2016).
 [26] M. Ablikim *et al.* (BESIII Collaboration), *Phys. Rev. Lett.* **125**, 052004 (2020).
 [27] M. Ablikim *et al.* (BESIII Collaboration), *Chin. Phys. C* **46**, 074001 (2022).
 [28] M. Ablikim *et al.* (BESIII Collaboration), *Nucl. Instrum. Meth. A* **614**, 345 (2010).
 [29] X. Y. Zhou, S. X. Du, G. Li and C. P. Shen, *Comput. Phys. Commun.* **258**, 107540 (2021).
 [30] D. J. Lange, *Nucl. Instrum. Meth. A* **462**, 152 (2001); R. G. Ping, *Chin. Phys. C* **32**, 599 (2008).
 [31] J. C. Chen, G. S. Huang, X. R. Qi, D. H. Zhang and Y. S. Zhu, *Phys. Rev. D* **62**, 034003 (2000); R. L. Yang, R. G. Ping and H. Chen, *Chin. Phys. Lett.* **31**, 061301 (2014).
 [32] M. Ablikim *et al.* (BESIII Collaboration), *Nature Phys.* **15**, 631-634 (2019).
 [33] J. Marraffino, S. Reucroft, C. E. Roos, J. Waters, M. Webster, A. Manz, R. Settles and G. Wolf, *Phys. Rev. D* **21**, 2501 (1980).
 [34] M. Ablikim *et al.* (BESIII Collaboration), *Phys. Rev. D* **87**, 012002 (2013).